



**HAL**  
open science

## Characterization of a depleted monolithic pixel sensors in 150 nm CMOS technology for the ATLAS Inner Tracker upgrade

F.J. Iguaz, F. Balli, M. Barbero, S. Bhat, P. Breugnon, I. Caicedo, Z. Chen,  
Y. Degerli, S. Godiot, F. Guilloux, et al.

### ► To cite this version:

F.J. Iguaz, F. Balli, M. Barbero, S. Bhat, P. Breugnon, et al.. Characterization of a depleted monolithic pixel sensors in 150 nm CMOS technology for the ATLAS Inner Tracker upgrade. 14th Pisa Meeting on Advanced Detectors, May 2018, La Biodola-Isola d'Elba, Italy. pp.652-653, 10.1016/j.nima.2018.11.009 . hal-01827996

**HAL Id: hal-01827996**

**<https://hal.science/hal-01827996>**

Submitted on 25 Oct 2021

**HAL** is a multi-disciplinary open access archive for the deposit and dissemination of scientific research documents, whether they are published or not. The documents may come from teaching and research institutions in France or abroad, or from public or private research centers.

L'archive ouverte pluridisciplinaire **HAL**, est destinée au dépôt et à la diffusion de documents scientifiques de niveau recherche, publiés ou non, émanant des établissements d'enseignement et de recherche français ou étrangers, des laboratoires publics ou privés.



Distributed under a Creative Commons Attribution - NonCommercial 4.0 International License

## NIMA POST-PROCESS BANNER TO BE REMOVED AFTER FINAL ACCEPTANCE

# Characterization of a depleted monolithic pixel sensors in 150 nm CMOS technology for the ATLAS Inner Tracker upgrade

F.J. Iguaz<sup>a,\*</sup>, F. Balli<sup>a</sup>, M. Barbero<sup>c</sup>, S. Bhat<sup>c</sup>, P. Breugnon<sup>c</sup>, I. Caicedo<sup>b</sup>, Z. Chen<sup>c</sup>, Y. Degerli<sup>a</sup>, S. Godiot<sup>c</sup>, F. Guilloux<sup>a</sup>, C. Guyot<sup>a</sup>, T. Hemperek<sup>b,1</sup>, T. Hirono<sup>b,1</sup>, H. Krüger<sup>b,1</sup>, J.P. Meyer<sup>a</sup>, A. Ouraou<sup>a</sup>, P. Pangaud<sup>c</sup>, P. Rymaszewski<sup>b,1</sup>, P. Schwemling<sup>a</sup>, M. Vandenbroucke<sup>a</sup>, T. Wang<sup>b</sup>, N. Wermes<sup>b,1</sup>

<sup>a</sup>IRFU, CEA, Université Paris-Saclay, F-91191 Gif-sur-Yvette, France

<sup>b</sup>University of Bonn, Nussallee 12, Bonn, Germany

<sup>c</sup>Centre de physique des particules de Marseille (CPPM), 163 Avenue de Luminy, Marseille, France

### Abstract

This work reports on design and performance of a depleted monolithic active pixel sensor (DMAPS) prototype manufactured in the LFoundry 150 nm CMOS process. DMAPS exploit high voltage and/or high resistivity inclusion of modern CMOS technologies to achieve substantial depletion in the sensing volume. The device used in this work, named LF-Monopix, was designed as a proof of concept of a fully monolithic sensor capable of operating in the environment of outer layers of the ATLAS Inner Tracker upgrade in 2025 for the High Luminosity Large Hadron Collider (HL-LHC). This type of devices has a lower production cost and lower material budget compared to presently used hybrid designs. In this work, the chip architecture will be described followed by the characterization of the different pixel flavors with an external injection signal and an iron source (5.9 keV x-rays).

**Keywords:** Depleted monolithic CMOS active pixel sensor, pixel detector, silicon detector

### 1. Introduction

LF-Monopix chip [1, 2] is the first fully monolithic prototype of Depleted Monolithic Active Pixel Sensors (DMAPS) [3] implemented in the LFoundry 150 nm CMOS technology aimed for high radiation environment. Its design has kept significant features from its ancestor LF-CPIX [4]. The chip size is  $1 \times 1 \text{ cm}^2$ , most of the device area is occupied by the pixel matrix composed of 36 columns and 129 rows. The pixel size is  $250 \mu\text{m} \times 50 \mu\text{m}$ . The pixel matrix is not uniform (see Fig. 1) and includes nine pixel flavors (four columns per flavor).

The different pixel types are built by combinations of pre-amplifier (NMOS or CMOS input), discriminator (a two stage open-loop structure, called V1; and a self-biased differential amplifier with a CMOS output stage, called V2), type of logic gate and placement of in-pixel readout logic. This work describes the characterization of the chip performance of three

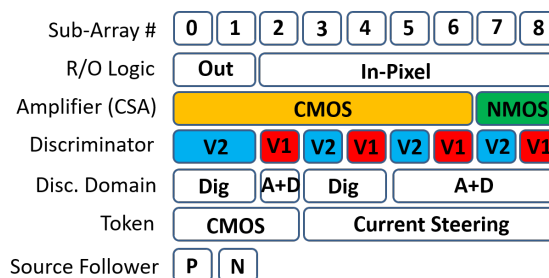


Figure 1: Blocs functional layout of LF-Monopix chip

samples (numbered 7, 11 and 12) in terms of breakdown voltage, gain, input capacitance, threshold dispersion and noise. LF-Monopix chip has also been tested under irradiation [5].

### 2. Characterization of chip performance

The first measured parameter of LF-Monopix chip is the breakdown voltage, which is the maximum voltage at which the detector can operate. This value is measured from the change

\*Corresponding author

Email address: [iguaz@cea.fr](mailto:iguaz@cea.fr) (F.J. Iguaz)

<sup>1</sup>Also in Physikalisches Institut der Universität Bonn, Nussallee 12, Bonn, Germany

of slope of the IV curve, the leakage current collected as a function of the reverse bias voltage applied to the outer P-Well guard rings, shown in Fig. 2. Values for breakdown voltage between 280 and 300 V were obtained, much higher than previous chip generation in the same technology [6]. This improved performance has been achieved by optimizing the guard ring structure based on TCAD simulations [7].

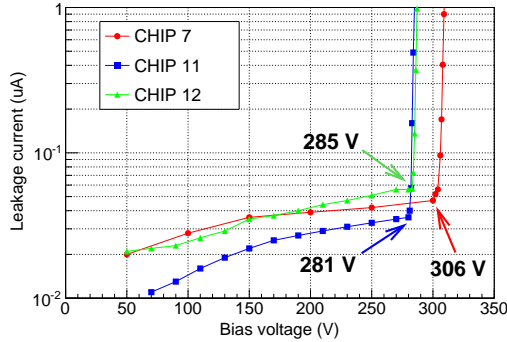


Figure 2: IV curves for three different samples of the LF-monopix chip at room temperature (20 degrees).

The gain of different pixels was calibrated using a  $^{55}\text{Fe}$  source (5.9 keV x-rays) and monitoring the response of individual pixels in the oscilloscope. For each pixel, the histograms of the signal amplitude and the baseline have been recorded and their mean values were measured. The pixel gain was then calculated as the ratio of the difference between these average values and the mean number of ion-electron pairs created by a 5.9 keV x-ray (1620 electrons). This procedure was repeated for a minimum of 8 pixels for each flavor. As shown in Table 1, only a dependence on the type of preamplifier was observed. Note that these gain values have to be considered as qualitative, since the real gain of the analogue chip chain is not precisely known. Nevertheless, the signal response of individual pixels can be used to estimate the input capacitance, by calculating the injection signal that gives the same signal response. The values obtained also show a dependence on the type of preamplifier.

Table 1: The performance of the two chip samples characterized in this work, in terms of gain and input capacitance (C).

#	Gain ( $\mu\text{V}/e$ )		Capacitance (fF)	
	CMOS	NMOS	CMOS	NMOS
7	$15.9 \pm 0.1$	$12.0 \pm 0.1$	$2.40 \pm 0.05$	$2.82 \pm 0.05$
12	$15.5 \pm 0.1$	$13.0 \pm 0.1$	$2.25 \pm 0.06$	$2.47 \pm 0.08$

The threshold distribution and noise level are studied by scanning an external injection signal into the sensing node and recording the probability of pixel firing with a fixed threshold setting, obtaining the so-called ‘‘S-curves’’. The threshold and noise parameters of each pixel are extracted by fitting an error function to the resulting S-curve. The scan results are shown in Table 2. The threshold level is  $\sim 2960$  ( $\sim 4300$ ) electrons for the V1 (V2) discriminator and its dispersion is  $\sim 530$  ( $\sim 930$ ) electrons. Meanwhile, the noise level is  $\sim 230$  ( $\sim 190$ ) electrons for CMOS (NMOS) preamplifier.

Table 2: The threshold, threshold dispersion and noise in electrons units before and after threshold tuning for different types of discriminator (in the first two cases) and preamplifier (in the last one). The TRIM value of all pixels is set to 0 for the untuned chip, while the TRIM distribution of each flavor is centered in 7 for the tuned chip. In all cases, the global threshold is set to 0.795 V.

Feature	Type	Untuned	Tuned
Threshold	V1 discri	$2960 \pm 150$	$4520 \pm 220$
	V2 discri	$4290 \pm 230$	$6000 \pm 250$
Thr. Disp.	V1 discri	$533 \pm 45$	$104 \pm 14$
	V2 discri	$926 \pm 89$	$153 \pm 21$
Noise	CMOS	$230 \pm 17$	$238 \pm 17$
	NMOS	$193 \pm 10$	$195 \pm 13$

The threshold of each pixel can be independently modified by a 4-bit in-pixel digital-to-analog converter (DAC) called TRIM. Therefore, each pixel was tuned by scanning the TRIM values, determining the corresponding threshold and fitting a linear relation between the TRIM values and the thresholds. Then the optimal TRIM for each pixel is set such as to minimize the threshold dispersion. The threshold dispersion is reduced down to  $\sim 150$  ( $\sim 100$ ) electrons for the V1 (V2) discriminator, while noise levels remain the same.

### 3. Summary

The performance of the different flavors of LF-Monopix chip has been characterized with an external injection signal and an iron source. The best results are obtained for the V1 discriminator (threshold dispersion of  $\sim 100$  electrons) and the NMOS preamplifier (noise level of  $\sim 190$  electrons). All chip samples show breakdown voltages between 280 and 300 V.

### Acknowledgments

This work has received funding from the European Union’s Horizon 2020 Research and Innovation programme under Grant Agreements no. 654168 (AIDA 2020) and 675587 (STREAM). F.J. Iguaz acknowledges the support from the Enhanced Eurotalents program (PCOFUND-GA-2013-600382).

### References

- [1] T. Wang et al., *Development of a Depleted Monolithic CMOS Sensor in a 150 nm CMOS Technology for the ATLAS Inner Tracker Upgrade*, *JINST* **12** (2017) C01039, [1611.01206].
- [2] T. Wang et al., *Depleted fully monolithic CMOS pixel detectors using a column based readout architecture for the ATLAS Inner Tracker upgrade*, *JINST* **13** (2018) C03039, [1710.00074].
- [3] I. Peric, *A novel monolithic pixelated particle detector implemented in high-voltage CMOS technology*, *Nucl. Instrum. Meth.* **A582** (2007) 876–885.
- [4] Y. Degerli et al., *Pixel architectures in a HV-CMOS process for the ATLAS inner detector upgrade*, *JINST* **11** (2016) C12064.
- [5] T. Hirono et al., *Depleted Fully Monolithic Active CMOS Pixel Sensors (DMAPS) in High Resistivity 150 nm Technology for LHC*, **1803.09260**.
- [6] T. Hirono et al., *CMOS pixel sensors on high resistive substrate for high-rate, high-radiation environments*, *Nucl. Instrum. Meth.* **A831** (2016) 94–98.
- [7] J. Liu et al., *Simulations of depleted CMOS sensors for high-radiation environments*, *JINST* **12** (2017) C11013.